Biochimica et Biophysica Acta 1777 (2008) 1173–1183

Contents lists available at ScienceDirect

Biochimica et Biophysica Acta

journal homepage: www.elsevier.com/locate/bbabio

Competition between linear and cyclic electron flow in plants deficient in Photosystem I

Simon Hald [a], Mathias Pribil [b], Dario Leister [b], Patrick Gallois [a], Giles N. Johnson [a,*]

[a] Faculty of Life Sciences, University of Manchester, Michael Smith Building, Oxford Road, Manchester, M13 9PT, UK
[b] Lehrstuhl für Botanik, Department Biologie I, Ludwig-Maximilians-Universität München, Menzinger Str. 67, 80638 München, Germany

ARTICLE INFO

Article history:
Received 28 January 2008
Received in revised form 20 March 2008
Accepted 28 April 2008
Available online 3 May 2008

Keywords:
Linear electron flow
Cyclic electron flow
Photosystem I
Photosystem II
PSI-D1
PSI-E1
Arabidopsis thaliana

ABSTRACT

Photosynthetic electron transport can involve either a linear flow from water to NADP, via Photosystems (PS) II and I or a cyclic flow just involving PSI. Little is known about factors regulating the relative flow through each of these pathways. We have examined photosynthetic electron transport through each system in plants of *Arabidopsis thaliana* in which either the PSI-D1 or PSI-E1 subunits of PSI have been knocked out. In both cases, this results in an imbalance in the turnover of PSI and PSII, such that PSII electron transport is limited by PSI turnover. Phosphorylation of light-harvesting complex II (LHCII) and its migration to PSI is enhanced but only partially reversible and not sufficient to balance photosystem turnover. In spite of this, cyclic electron flow is able to compete efficiently with PSI across a range of conditions. In dark-adapted leaves, the efficiency of cyclic relative to linear flow induced by far-red light is increased, implying that the limiting step of cyclic flow lies in the re-injection of electrons into the electron transport chain. Illumination of leaves with white light resulted in transient induction of a significant non-photochemical quenching in knockout plants which is probably high energy state quenching induced by cyclic electron flow. At high light and at low CO_2, non-photochemical quenching was greater in the knockout plants than in the wildtype. Comparison of PSI and PSII turnover under such conditions suggested that this is generated by cyclic electron flow around PSI. We conclude that, when the concentration of PSI is limiting, cyclic electron flow is still able to compete effectively with linear flow to maintain a high ΔpH to regulate photosynthesis.

1. Introduction

The Photosystem (PS) I complex of higher plants is a light driven enzyme that catalyzes the transfer of electrons from plastocyanin (PC) in the thylakoid lumen to ferredoxin (Fd) on the stromal side of the thylakoid membrane [1]. PSI lies at the centre of photosynthesis, catalysing the last membrane bound step of electron transport, and electrons transferred through the PSI complex can take part in a range of reactions. The primary pathway, linear electron transport, involves electron transfer via Fd and ferredoxin-$NADP^+$-oxidoreductase (FNR) to reduce $NADP^+$, generating NADPH which provides reducing potential for the Benson–Calvin cycle and other metabolic processes. Alternatively, electrons can be transferred from the acceptor side of PSI to oxygen, the Mehler reaction [2]. The extent and significance of this reaction is debated [3], however it is likely that it contributes significantly to oxidative stress in leaves under some conditions. In addition, a cyclic electron transport pathway, involving the return of electrons from the acceptor side of PSI to the donor side, is thought to play an essential role in photosynthesis (for reviews see [4,5]). Given this central role for PSI and its potential to influence the partitioning of electrons between different processes, an understanding of its functioning in the context of whole chain electron transport is essential.

PSI is a multisubunit complex [1] composed of 15 core subunits, PSI-A to -L and PSI-N to -P. This core is associated with light-harvesting complex I (LHCI) consisting of four subunits, Lhca1 to Lhca4. All subunits are transmembrane, except PSI-C, -D, -E and -N. PSI-N is soluble in the lumen, and PSI-C, -D and -E are extrinsically membrane bound on the stromal side. The latter three form a compact interconnected structure, known as the stromal ridge. PSI-C is necessary for the stable association of PSI-D and -E [6].

PSI-D and PSI-E each occur in two isoforms, termed PSI-D1, -D2, -E1 and -E2. Each isoform has been studied by knockout mutation in *Arabidopsis thaliana* plants. Ihnatowicz et al. [7] showed, by knocking out each isoform of PSI-D in *Arabidopsis*, that the major effect rested with the D1 isoform. Knockout plants lacking PSI-D1 exhibited stunted growth and had only approximately 40% accumulation of the PSI core complex per unit chlorophyll compared to the wildtype. Plants had impaired photosynthesis under low light conditions, and increased photosensitivity. Accumulation of PSII was reduced to approximately 70% of wildtype. A PSI-D2 knockout, on

Abbreviations: cyt, cytochrome; Fd, ferredoxin; FNR, ferredoxin-$NADP^+$-oxidoreductase; LHC, light-harvesting complex; NPQ, non-photochemical quenching; PC, plastocyanin; PS, photosystem

* Corresponding author. Tel.: +44 161 275 5750; fax: +44 161 275 5082.
E-mail address: giles.johnson@manchester.ac.uk (G.N. Johnson).

0005-2728/$ – see front matter © 2008 Elsevier B.V. All rights reserved.
doi:10.1016/j.bbabio.2008.04.041

the other hand, had no detectable phenotype. Haldrup et al. [8] demonstrated that antisense suppression of PSI-D is accompanied by a similar reduction of the PSI complex, but not the PSII and cytochrome (cyt)b_6f complexes. The major isoform of PSI-E, the E1 isoform, has also been studied by knockout mutation, with knockout plants having stunted growth, a marked reduction in most PSI subunits, and impaired photosynthesis under low light conditions [9]. PSI-E1 has been proposed to have a role in state transitions, as a stable LHCII-PSI aggregate was responsible for the suppression of state transitions in mutant plants lacking PSI-E1 [10,11].

Plants deficient in either PSI-D1 or -E1 are similar in many aspects, but there is a notable difference in suppression of proteins of the PSI complex. In the PSI-D1 knockout line, 60% of the entire PSI-D is knocked out, as evidenced by immunoblotting [7]. This is accompanied by similar reduction in the accumulation of the entire core PSI complex, together with the associated LHCI. In PSI-E1 knockout lines, a similar loss of the E1 protein itself is seen, but the mutant retains wildtype levels of PSI-A, -B and -F, as well as Lhca1 to Lhca4. This core complex probably retains some functionality as plants with both PSI-E isoforms knocked out retain some ability to grow photosynthetically [12]. Regardless of these differences, both knockout lines can be characterized as being PSI-limited, that is they exhibit reduced activity of PSI, leading to an imbalance in the stoichiometry of PSI to PSII in the favour of PSII.

Given their location on the acceptor side of PSI, PSI-D and -E are thought likely to play a role in influencing the fate of electrons passing through PSI. In cyanobacteria, PSI-E has been suggested to be essential for cyclic electron flow [13], although recent data questions this conclusion [14]. Recently, Breyton et al. [15] examined the regulation of cyclic electron flow in wildtype *Arabidopsis* and discussed various models that might determine the partitioning between linear and cyclic flows, with different degrees of segregation between the two pathways being assumed. At one extreme, cyclic flow might take place in supercomplexes, comprising PSI, cyt b_6f, Fd and PC, however no biochemical evidence for this model has been found [15]. At the other extreme, simple competition might occur between the two pathways. Various other models, assuming different degrees of segregation can also be postulated. In particular, competition might depend on the distribution of FNR between membrane bound and soluble forms or between PSI-bound and cyt b_6f-bound forms.

Irrespective of which model is correct, the pivotal role of PSI is obvious. However, none of the proposed models outline the importance of the stoichiometric balance of PSI to PSII, or what effect an imbalance would have on the occurrence of cyclic electron flow. In this communication, we addressed this question by investigation of PSI-limited transgenic *Arabidopsis* lines, having either PSI-D1 or -E1 knocked out. We present evidence that cyclic electron transport still occurs in these lines, and that it proceeds at a proportionally higher

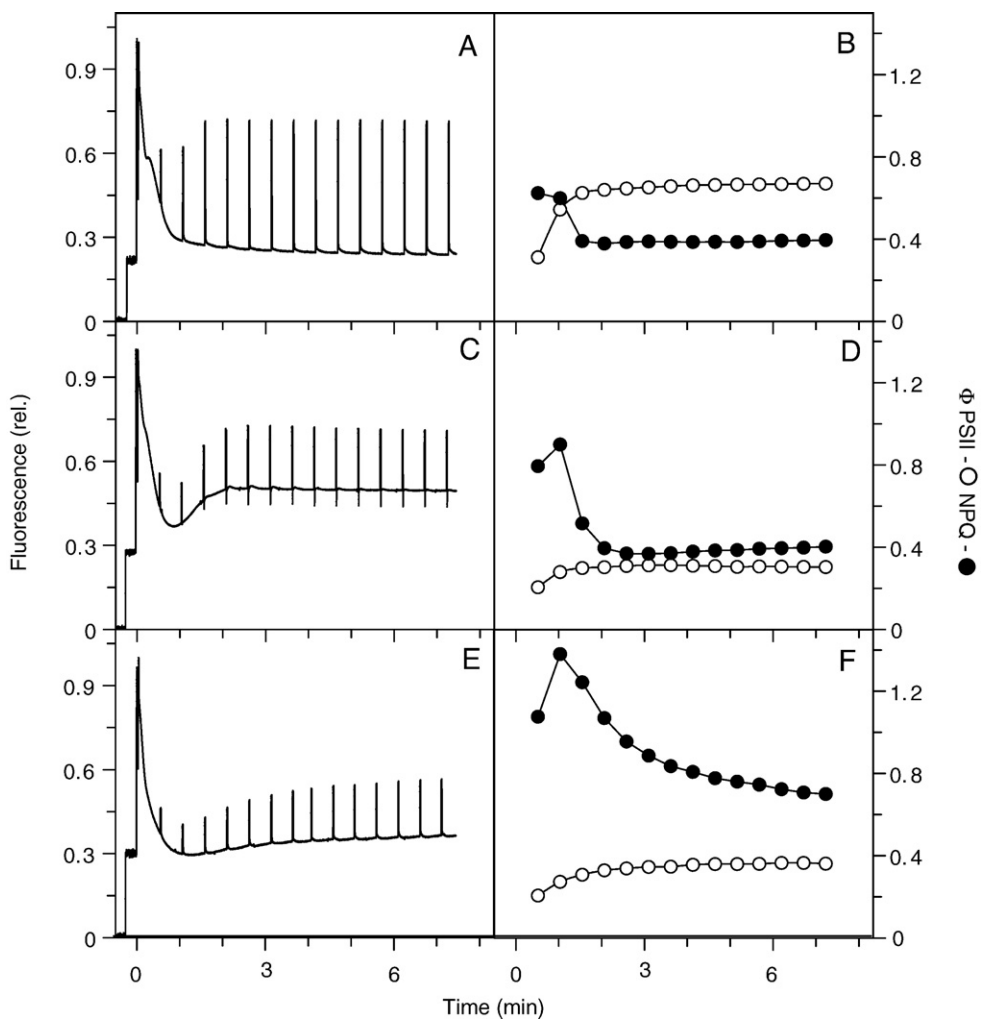

Fig. 1. Chlorophyll fluorescence induction in plants of wildtype (A,B), *psad1-1* (C,D) and *psae1-3* (E,F) lines illuminated at 150 μmol m^{-2} s^{-1} at 20% oxygen and 2000 μl l^{-1} CO_2. A saturating flash (8000 μmol m^{-2} s^{-1}) was applied each at 30 s. A;C;E—Representative fluorescence traces are shown for wildtype (A), *psad1-1* (C) and *psae1-3* (E) lines. B; D; F—Changes in Φ_{PSII} and NPQ measured from the fluorescence traces shown.

rate, relative to linear electron transport, than is the case in wildtype plants under low light conditions. Furthermore, we demonstrate that plants without PSI-D1 or -E1 have capacity for cyclic electron transport under stress conditions, such as high light or CO_2 limitation.

2. Materials and methods

2.1. Plant growth

Seeds from wildtype (Col-0) *Arabidopsis* plants and from PSI-D1 [7] and PSI-E1 [12] knockout lines were sown in soil, and plants were grown in a controlled-environment growth chamber with a photon flux density (PFD) of 150 μmol m^{-2} s^{-1} on a 8 h light/16 h night regime. Day temperature was 20 °C and night temperature was 16 °C. Fully expanded, intact leaves of 8–10 week old plants were used for analysis.

2.2. Gas exchange, light response, P700 oxidation and chlorophyll fluorescence measurements

Plants were dark-adapted overnight prior to each measurement. For steady-state measurements of photosynthetic parameters, attached leaves were clamped into the chamber of an infra-red gas analyser (IRGA) (PP Systems, Hitchin, UK), which enabled the external CO_2 concentration to be controlled, whilst the internal CO_2 concentration (C_i) could be calculated from gas exchange parameters. Pure nitrogen and oxygen were supplied by gas cylinders (BOC, Guildford, UK). Nitrogen and oxygen gas flow rates were controlled by MKS mass flow controllers connected to an MKS model PR 4000 controller (MKS Instruments, Massachusetts, USA). This allowed the oxygen concentration to be controlled. Light response measurements were carried out at ambient oxygen and the external CO_2 concentration was set to 2000 μl l^{-1}.

Changes in absorbance at 830 nm were used as a measure of the redox state of P700, the primary PSI donor. Measurements were made using a Walz PAM 101 fluorometer with an ED-P700DW-E emitter-detector unit (Walz, Effeltrich, Germany). Actinic light was supplied by an Intralux 6000 lamp (Volpi, Schlieren, Switzerland) filtered by a Calflex-X filter. Chlorophyll fluorescence measurements were made using a PAM 101 fluorometer together with a 101-ED emitter-detector unit (Walz, Effeltrich, Germany). Saturating pulses of light (8000 μmol m^{-2} s^{-1}) were supplied by a Volpi Intralux 1500 lamp (Volpi). Lights were shuttered using a Uniblitz 14 mm electronic shutter (Vincent Associates, Rochester, N.Y., USA), controlled by a computer using laboratory-written software.

Measurements of PSII parameters were calculated as described by Maxwell and Johnson [16], where $\Phi_{PSII}=(F_m'-F_t)/F_m'$ and $NPQ=(F_m-F_m')/F_m'$. Calibration of the maximum P700 signal size, measurements of chlorophyll fluorescence and measurements of $P700^+$ were performed as described by Golding and Johnson [17]. Measurements of the light and CO_2 response curve were obtained using a new leaf for each measurement at each of the different light intensities and CO_2 concentrations, respectively.

2.3. Quenching relaxation analysis

PSI-D1 and PSI-E1 knockout and wildtype plants were dark-adapted overnight before being clamped into the cuvette chamber of the IRGA. Leaves were subjected to light for 30 min and chlorophyll fluorescence parameters were recorded. Then, light was turned off and every 120 s a 1 s flash of saturating light was given for a period of 30 min. Actinic irradiance was at 1500 μmol m^{-2} s^{-1}.

2.4. Membrane potential measurements

Spectroscopic measurements of membrane potential changes were performed on intact leaves of overnight dark-adapted plants with a flash spectrophotometer as described previously [15,18]. Briefly, membrane potential changes were measured at 520 nm using a white LED source (Luxeon, Lumileds) filtered through appropriate interference filters. Preflashes were provided by a green LED source (λ_{max}=530 nm). Far-red illumination was provided by a high powered LED chip peaking at 740 nm (LED740-66-60, Roithner Lasertechik, Vienna, Austria), filtered through a Schott RG710 glass filter.

2.5. State transition measurements

State transitions were measured using a protocol similar to that described in [19]. Briefly, state transitions were measured on intact leaves with a PAM fluorometer. The leaf was subjected to a saturating flash for 1 s followed by illumination for 34 min at 30 μmol m^{-2} s^{-1} of blue light (Luxeon LXHL-LB5C, λ_{max}=470 nm, Philips, LumiLed, USA). Then, the blue light was turned off and replaced by far-red light (LED740-66-60, Roithner Lasertechnik, Austria, filtered by a Schott RG-715 glass filter) for 28 min. The far-red light was turned off and fluorescence was measured again in the blue light for 20 min. Every fourth minute, a saturating 1 s flash was applied, allowing for subsequent calculation of Φ_{PSII} and NPQ.

2.6. Immunoblot analysis

Leaves from plants, adapted to the different light conditions used to monitor state transitions (dark, blue or far-red light; see above), were harvested and frozen in liquid nitrogen. Thylakoids were prepared in the presence of 10 mM NaF and fractionated on a SDS-polyacrylamide gradient gel, as previously described [20]. After blotting, filters were probed with phosphothreonine-specific antibodies (Cell Signalling) and signals were detected by enhanced chemiluminescence (Amersham Biosciences). To control equal loading filters were immunolabelled with antibodies raised against Lhcb2.

3. Results

3.1. Responses of PSII parameters to low light

Exposure of a dark-adapted wildtype *Arabidopsis* leaf to 150 μmol m^{-2} s^{-1} white light, in the presence of saturating CO_2 and ambient oxygen, resulted in a rapid rise in fluorescence, followed by a slower quenching, with fluorescence reaching a steady-state yield close to F_o (Fig. 1). Fluorescence quenching analysis revealed an initial, transient increase of NPQ, as has been described previously [21], this being replaced by photochemical quenching upon prolonged illumination, such that the steady-state fluorescence level (F_t) fell throughout the induction period. In both *psad1-1* and *pase1-3* lines, illumination resulted in a steady-state level of fluorescence that fell from an initial peak, to reach a minimum at approximately 100 s, after which F_t rose again reaching a steady level that was significantly higher than F_o. Quenching analysis revealed that this transient quenching was due to the induction of a high level of NPQ. As in the wildtype, this transient quenching relaxed upon prolonged illumination, however, it was not replaced by photochemical quenching. The maximum Φ_{PSII} attained in the two mutant lines was similar, but substantially lower than in wildtype.

The responses of *psad1-1* and *psae1-3* plants to low light illumination were overall quite similar. Nevertheless, certain differences were observed. Application of a saturating flash to *psad1-1* leaves resulted in a negative transient in the fluorescence yield following a return to actinic light, a phenomenon absent in both the wildtype and the *psae1-3* mutant. Closer examination of the fluorescence transient during and after a flash revealed that the flash induced a quenching of F_m, which might be related either to the flash-induced generation of a ΔpH, leading to NPQ, or flash-induced accumulation of reduced pheophytin. Measurements with a lower flash intensity tended to reduce the extent of this phenomenon, but were however less saturating. The F_m values measured in the PSI-D1 lines under these conditions are liable to be a slight underestimation, leading to an exaggeration of NPQ and an underestimation of Φ_{PSII}. This phenomenon was only present when low intensities of actinic light were used.

3.2. Migration of phosphorylated LHCII to PSI occurs in psad1-1 and psae1-3 mutants but is not sufficient to balance PSI to PSII turnover at low light

The high steady-state level of F_t observed in the *psad1-1* and *psae1-3* lines in Fig. 1 results from a suppression of Φ_{PSII}, which is not compensated for by an increase in NPQ over wildtype levels. The drop in Φ_{PSII} at limiting light intensities implies an imbalance in the turnover of PSI and PSII, such that the electron transport chain, in particular the plastoquinone pool, is maintained in a reduced state. In wildtype plants, imbalances in PSI:PSII turnover at low light are thought to be compensated for by the process of state transitions [22,23]. State transitions can be observed as giving rise to a non-photochemical quenching of chlorophyll fluorescence (NPQ_T). Previously, a marked suppression of reversible state transitions was observed in PSI-D1 and -E1 knockout lines [7,10], indicating impairment in the re-distribution of excitation energy between the photosystems.

In order to determine whether state transitions might contribute to low light NPQ, we examined fluorescence quenching parameters by using a protocol modified from [19]. In contrast to that previous work, dephosphorylation of LHCII was induced by applying a pure far-red light, and not by imposing it on a PSII favouring light. We have made estimates of state transitions using LED light sources, which have a narrow spectral range. Sustained illumination with low-intensity blue

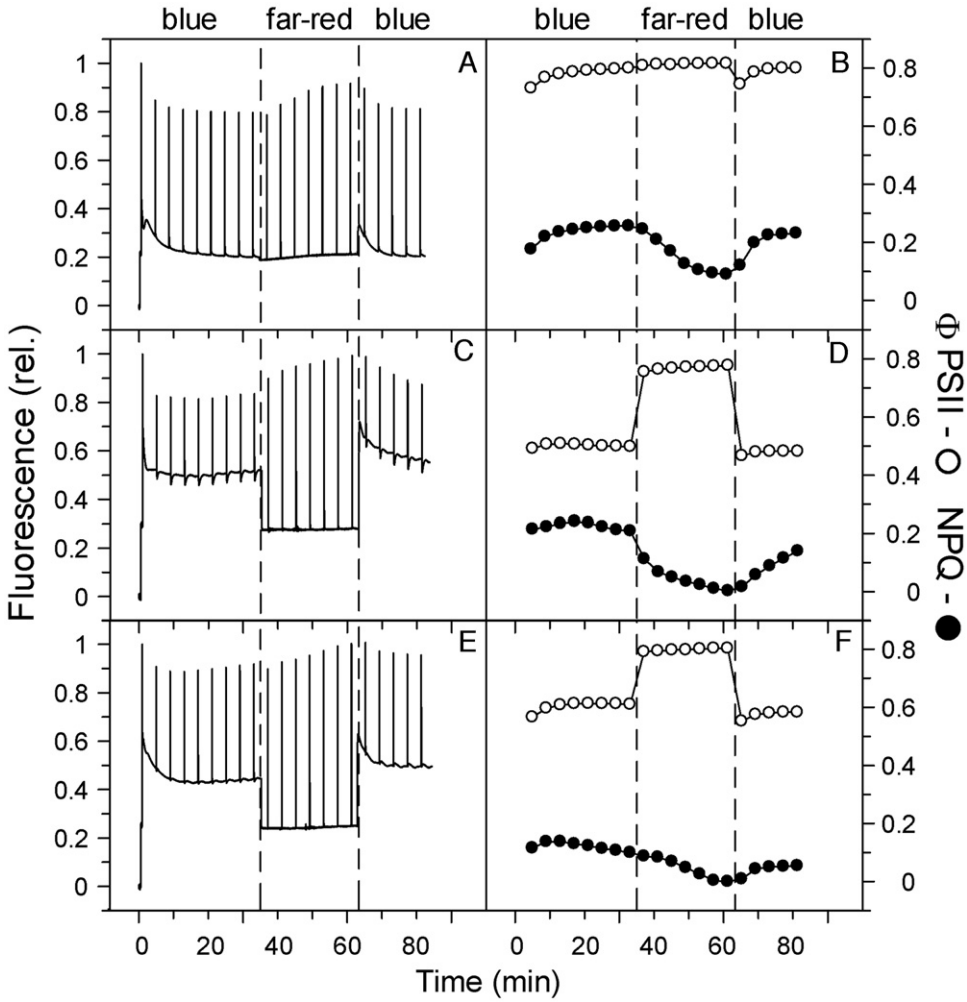

Fig. 2. The occurrence of state transitions, as monitored by chlorophyll fluorescence in wildtype (A,B), *psad1-1* (C,D) and *psae1-3* (E,F) lines. Dark-adapted leaves were exposed to low-intensity blue light (λ_{max}=470 nm, 30 μmol m^{-2} s^{-1}). After 35 min, light was changed to far-red (λ_{max}=710 nm). After a further 20 min this light was switched back to blue. A saturating flash (8000 μmol m^{-2} s^{-1}) was applied 4 min throughout the experiment. A;C;E—Representative fluorescence traces are shown for wildtype (A), *psad1-1* (C) and *psae1-3* (E) lines. B; D; F—Changes in Φ_{PSII} and NPQ measured from the fluorescence traces shown. Dashed lines indicate the change of light source.

light (λ_{max}=530 nm) resulted in a slow induction of NPQ in all plants, with a steady-state level of approximately 0.2 being achieved (Fig. 2). In wildtype, the steady-state value of F_t was close to F_o. In both mutant lines, an F_t value significantly higher than F_o was observed. This implies that, whilst in wildtype state transitions are able to balance photosystem excitation, this was not the case in the mutant lines. This might either be because no state transition was occurring or because it was insufficient to balance the turnover of the two photosystems. When the light source was switched from blue to far-red, there was an immediate substantial drop in the F_t in both mutant lines, implying that an oxidation of the plastoquinone pool is induced. This effect is largely absent in wildtype plants. Prolonged exposure to far-red light resulted in a decline in NPQ in all the plants measured. This is consistent with all plants exhibiting a state transition in blue light that is reversed by far-red light. Shifting from far-red back to blue light, the plastoquinone pool rapidly became over-reduced in all plants, as indicated by the transient rise in fluorescence. Shortly thereafter F_t relaxed to the level seen at the end of the initial blue-light illumination, this being high in the knockout lines.

Under initial illumination with blue light, Φ_{PSII} was clearly higher for the wildtype than for the *psad1-1* and *psae1-3* lines. Φ_{PSII} is only transiently affected by the alternation between PSII- and PSI-exciting light in the wildtype, whereas both knockout lines had elevated Φ_{PSII} values, similar to that of the wildtype when subjected to far-red light alone. In all plants, steady-state values of NPQ were similar under all conditions, with this being highest under blue light and dropping upon illumination with far-red light. We suggest that this blue-light induced NPQ is due to state transitions occurring in all plants, with this being reversed upon far-red illumination.

Previously, Ihnatowicz et al. [24] observed that imposing far-red light on background blue light did not result in the full dephosphorylation of light-harvesting proteins, suggesting that state transitions were not

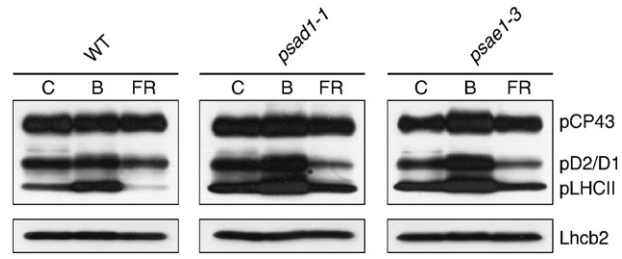

Fig. 3. Thylakoid protein phosphorylation levels in WT and mutants (*psad1-1* and *psae1-3*) adapted to the different light conditions used to monitor state transitions. The phosphorylation levels of CP43 (pCP43), D1/D2 (pD1/D2) and LHCII (pLHCII) were detected by Western analysis using a phosphothreonine-specific antibody (upper panels). The same filters were immunolabelled with Lhcb2-specific antibodies to control equal loading (lower panels). C, dark-adapted; B, blue-light adapted; FR, far-red light adapted.

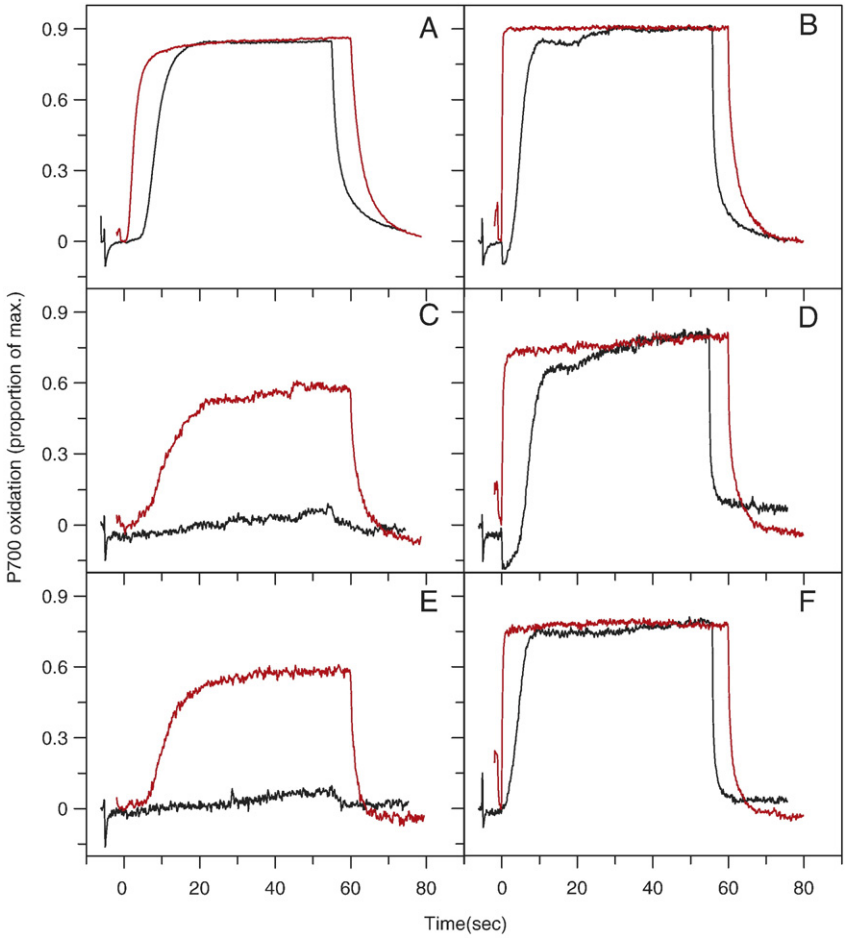

Fig. 4. Effect of far-red illumination on the redox state of P700 in dark-adapted and pre-illuminated leaves of wildtype (A, B), *psad1-1* (C, D) and *psae1-3* (E, F) lines. Dark-adapted leaves were exposed to a 200 ms flash of saturating light and then, after 5 s, a far-red light was applied (black traces). The same leaves were then exposed to an actinic light (200 μmol m^{-2} s^{-1}) for 20 min. Leaves were then darkened for 1 s before reapplication of far-red light (red traces). In all cases scale has be set for far-red light on at t=0 s. Far-red intensity was either low (A,C,E), or high (B,D,F) with the low intensity being 5% of the high intensity. All traces are normalised to the maximum signal recorded in leaves that were illuminated and then re-darkened for 5 min.

fully reversed. To confirm that this is also the case when leaves are illuminated with far-red light alone, where we are confident that the PQ pool is fully oxidised, we performed an assay of the phosphorylation state of thylakoid proteins in dark-adapted, blue-light illuminated and far-red light illuminated conditions (Fig. 3). As observed previously, in dark-adapted leaves there is a degree of phosphorylation of thylakoid proteins, which is increased upon illumination with blue light. Exposure to far-red light reverses this additional phosphorylation, however only to the extent seen in the dark-adapted leaves. A similar pattern was observed in D1/D2 and CP43 phosphorylation patterns. Thus we conclude that state transitions are only partially reversible in the *psad1-1* and *psae1-3* knockout mutants, indicating that only part of the marked drop in NPQ observed in mutant plants upon exposure to far-red light is attributable to the decrease in NPQ_T.

Knocking out either PSI-D1 or PSI-E1 goes beyond just removing the single protein from the PSI complex [7,9,10,12]. The secondary effect of each knockout is a marked reduction in the activity of and to a greater or lesser extent in the amounts of other polypeptides of the PSI complex, resulting in an imbalance in the stoichiometry of PSII to PSI in the favour of PSII. In line with earlier observations [7,10], our data (Fig. 2) indicate that the knockout lines are unable to balance the excitation between the two photosystems despite an enhanced phosphorylation of LHCII, that persists even after a prolonged exposure to far-red light. Thus, linear electron transport from PSII to PSI fails to operate efficiently in the PSI-D1 and -E1 lines, and this is due to the reduced amount of PSI.

3.3. Cyclic electron transport competes efficiently with linear in dark-adapted leaves in PSI-D1 and -E1 mutants

The transient appearance of NPQ under low light conditions (Fig. 1) has previously been explained by the generation and relaxation of a *trans*-thylakoid pH gradient [21]. The extent of this quenching, which is high compared with reported values for NPQ_T, as well as the observation that it relaxes, make it unlikely that state transitions contribute to this effect significantly and the reversibility rules out a contribution of photoinhibition. Following the initial exposure of a dark-adapted leaf to light, the *trans*-thylakoid pH gradient builds up, leading to an increase in NPQ. At this stage the NADPH- and ATP-consuming reactions of the Benson–Calvin cycle are inactive. Upon further illumination, NPQ reaches a peak and then begins to drop. This relaxation can be explained by the light activation of enzymes involved in carbon fixation in the Benson–Calvin cycle, which in turn results in the relaxation of the *trans*-thylakoid pH gradient [21].

Several processes might contribute to the transient generation of ΔpH upon illumination, including, in particular, electron transport to oxygen and cyclic electron transport around PSI. To investigate the contribution of the former process, measurements were performed at 2% oxygen (data not shown), and notably, the appearance of transient NPQ was also seen. This allows us to deduce that electron transport to oxygen does not play a substantial role in the generation of the *trans*-thylakoid pH gradient under these conditions. It thus seems likely that cyclic electron flow is the major contributor to transient ΔpH in all the

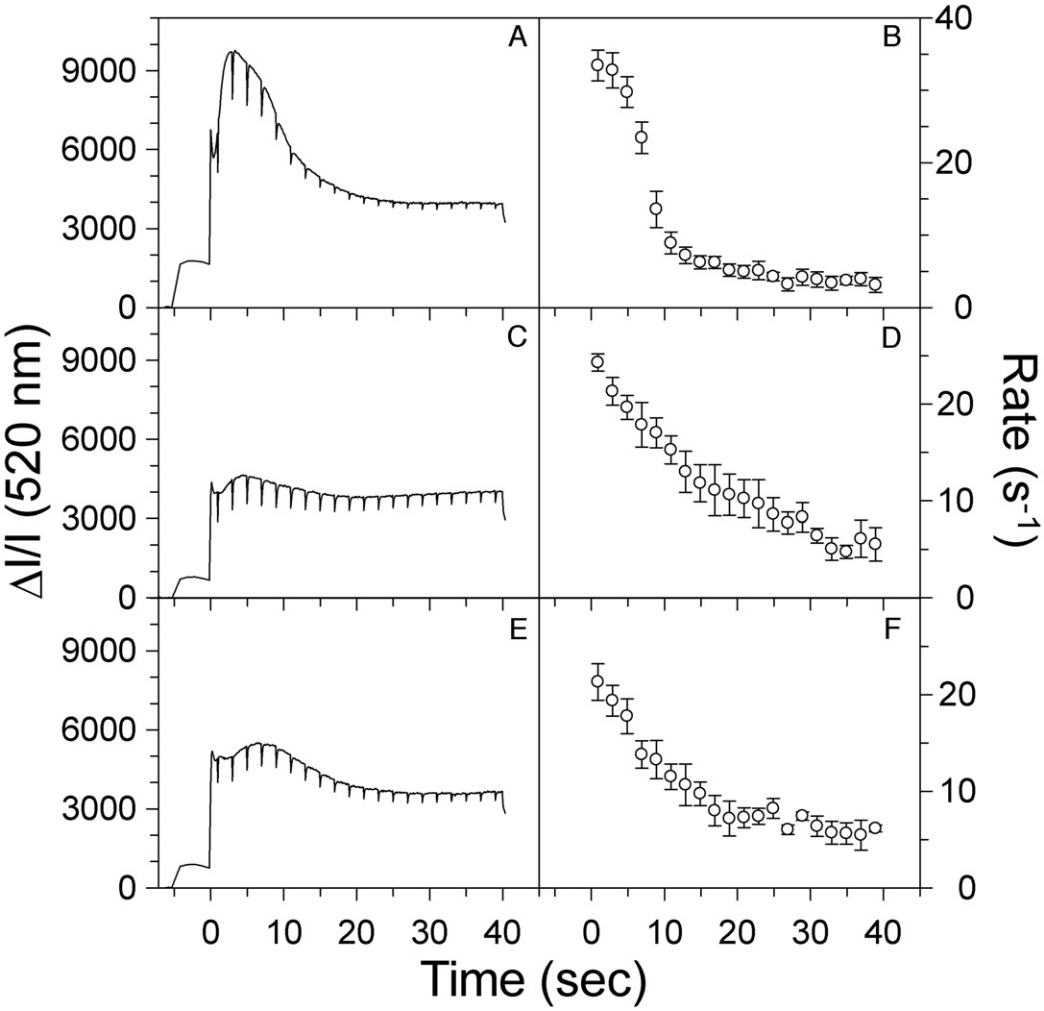

Fig. 5. Membrane potential changes induced by low-intensity far-red light in wildtype (A,B) and *psad1-1* (C,D) and *psae1-3* (E,F) lines. A;D;E—Representative traces of membrane potential changes. In each case a 200 ms saturating flash of light was applied at $t=-5.2$ s and far-red light applied from $t=0$ s. Far-red light was turned off for 50 ms after 0.9 s again after every 2 s of light. The dark-induced transients are visible as downward spikes. The intensity of far-red light was as in Fig. 4A. B;D;F—relative rates of charge separation. The difference in the slope of the membrane potential curves immediately before and after switching off the light for each dark period is shown as a measure of relative electron transport rate. Each point represents the mean±SE of at least three measurements on separate plants.

plants studied. Cyclic electron flow specifically requires activity of PSI and the two mutant lines were both deficient in PSI content. However, the extent of NPQ transiently induced in the two mutant lines was greater than that seen in wildtype, suggesting that a substantial ΔpH was being generated, in spite of the lack of PSI.

Recently, evidence for the occurrence of cyclic electron transport has been obtained by examining the kinetics of P700 oxidation using far-red light in either dark-adapted or pre-illuminated leaves [4,15]. Adopting the same approach, we compared the kinetics of P700 oxidation upon application of far-red light in wildtype and *psad1-1* and *psae1-3* plants (Fig. 4). Dark-adapted leaves were subjected to a 200 ms saturating flash of light, followed by a low-intensity far-red illumination for 60 s The same leaf was then subjected to actinic light for a period of 15 min (light-adapted), after which far-red illumination was re-applied and P700 oxidation monitored. In dark-adapted leaves of wildtype plants, P700 was readily oxidised, following a lag period of a few seconds. In contrast, in *psad1-1* and *psae1-3* lines, very little oxidation of P700 occurred under the same experimental conditions. Illumination with actinic light was then used to activate the enzymes of the Benson–Calvin cycle. Low-intensity far-red illumination of light-adapted leaves of wildtype plants led to rapid oxidation of P700 with the steady-state level being similar to that of dark-adapted leaves. P700 reached its maximum level of oxidation faster than in dark-adapted leaves, as there was no lag in the induction of P700 oxidation, a phenomenon which has been ascribed to the suppression of cyclic electron flow [4,15]. In contrast to dark-adapted leaves, light-adapted leaves of the two knockout lines showed clear oxidation of P700, although this was slow compared to their wildtype counterpart.

The lag and slow oxidation of P700 observed in wildtype plants has previously been ascribed to the occurrence of cyclic ET [4,15]. In dark-adapted leaves of the *psad1-1* and *psae1-3* lines, this lag was especially marked, with little or no net oxidation of P700 occurring. Furthermore, there was an obvious slowing down of P700 oxidation in the light-adapted leaves of the *psad1-1* and *psae1-3* lines, compared to the wildtype. Taken together, these observations might be an indication that proportionally more cyclic than linear electron transport is taking place in the mutant plants, when compared to the wildtype. However, various other explanations for this slow oxidation can also be suggested.

The imbalance in PSI:PSII in the mutant plants might mean that, even in the presence of far-red light, excitation of PSII exceeds that of PSI, meaning that no net oxidation of PSI will occur. Various lines of evidence allow us to exclude this possibility, however. Far-red illumination of leaves infiltrated with the herbicide DCMU, to block PSII turnover, did not result in a significant increase in the oxidation of P700 (not shown). Application of far-red light should give no oxidation of P700 even after activation of the Benson–Calvin cycle. This is not the case — in leaves

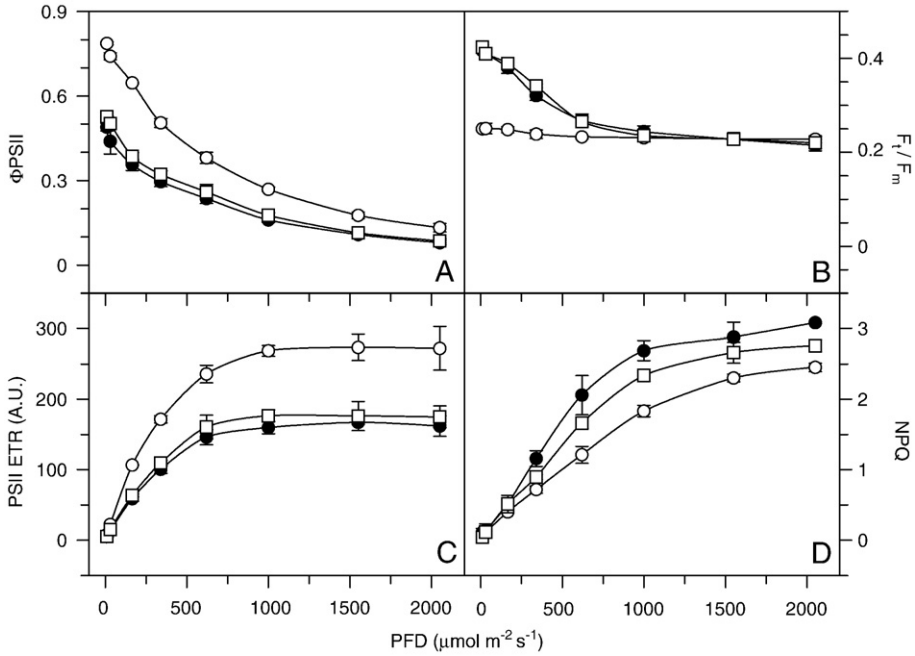

Fig. 6. Irradiance dependence of chlorophyll fluorescence quenching parameters in wildtype (○), *psad1-1* (●) and *psae1-3* (□) lines. Quantum yield of PSII (Φ_{PSII}; A), F_t/F_m ratios (B), relative electron transport through PSII (PSII ETR, C), and non-photochemical quenching (NPQ, D) were measured in plants subjected to a range of light intensities at 20% oxygen and 2000 μl l^{-1} CO_2. Leaves were illuminated for 30 min to allow photosynthesis to reach a steady state, before a saturating flash (8000 μmol m^{-2} s^{-1}) was applied to estimate fluorescence parameters. Each point represents the mean ± SE of at least three measurements on separate plants.

pre-illuminated with actinic light, P700 was readily oxidised (Fig. 4). Finally, an imbalance in PSI:PSII turnover would be expected to be independent of the intensity of far-red irradiance used or indeed to be worse under high far-red light, as PSI becomes light saturated before PSII. Upon application of a high-intensity far-red illumination (~20× that used previously), P700 was readily oxidised in all plants. This acceleration in oxidation is inconsistent with the idea that an imbalance in PSI:PSII turnover inhibits P700 oxidation under far-red light.

Early work from Siebke et al. [25] suggested that the slow oxidation of P700 by far-red light might be due to the net reduction of the PSI acceptor pool by electrons flowing through the electron transport chain, resulting in a transient blockage in overall electron flow. Thus, the failure of low far-red light to oxidise P700 might result from such an effect. In light-adapted leaves, where the Benson–Calvin cycle provides an efficient sink for reducing equivalents, P700 was rapidly oxidised in all plants, consistent with the idea that P700 oxidation is sink limited. However, this effect is again expected to occur, and even increase, with increased far-red light. Instead, increasing the far-red light intensity resulted in an acceleration of P700 oxidation, an effect that is inconsistent with reduction of the acceptor pool being responsible for the failure to oxidise P700.

Further evidence against a blockage in electron transport being responsible for the failure to oxidise P700 comes from measurements of the ability of plants to generate an electrical field across the thylakoid membrane, as indicated by the electrochromic shift in the region of 520 nm (Fig. 5). Dark-adapted leaves were subjected to low-intensity far-red illumination as in previous measurements. In wildtype, an initial rapid generation of the field is followed by a slower rise and then a decay over a period of approximately 10 s. In *psad1-1* and *psae1-3* plants, similar kinetics were observed, however the second rise and fall was less marked. Throughout the course of illumination, short dark pulses of 50 ms in duration were applied every 2 s. The transient shift from light to dark allows the estimation of the total photochemical rate (PSI + PSII) measured as the rate of the far-red light induced formation of the membrane potential [18]. The difference in the slopes immediately before and after light is switched off can be taken as an indication of this rate [26]. During the first few seconds of low-intensity far-red illumination, the rate is maintained at high levels in all plants. Thereafter, however, in wildtype plants the rate drops steeply and, within a few seconds, steady levels of approximately 10% of the initial rates are reached. On the other hand, in the *psad1-1* and *psae1-3* lines the rate drops much more slowly, and it appears that after the first ca. 30 s steady levels are reached, approximately 20% of the initial rates. From this we conclude that both the *psad1-1* and *psae1-3* lines maintain a rate of electron transport throughout the period when no net oxidation of P700 is occurring.

Based on the above observations, we conclude that, in dark-adapted leaves, the efficiency of cyclic electron transport around PSI is greater in *psad1-1* and *psae1-3* mutants than in wildtype.

3.4. Cyclic electron transport is able to compete efficiently with linear flow at high light

The occurrence of cyclic electron transport under stresses such as high light and low CO_2 is well documented [17,27,28]. We investigated the effect of varying light intensities on the *psad1-1* and *psae1-3* lines. Fluorescence quenching parameters were measured at a set of different irradiances in the presence of saturating CO_2 and at ambient oxygen (Fig. 6). As the irradiance increased, Φ_{PSII} dropped in all plants, reflecting progressive saturation of PSII. Φ_{PSII} was lower in both *psad1-1* and *psae1-3* lines than in wildtype plants at all irradiances (Fig. 6A). The degree of suppression of Φ_{PSII} was very similar in the two knockout lines. Electron transport through PSII (PSII ETR) was estimated as the product of Φ_{PSII} and irradiance (Fig. 6C). ETR in all plants saturated at around 600 μmol m^{-2} s^{-1}. As seen in Fig. 1, at low light the steady-state level of fluorescence, F_t, expressed relative to F_m was elevated compared to the wildtype (Fig. 6B). However, this was only true under conditions of light limitation. As irradiance rose above the saturation point for PSII electron transport, F_t/F_m fell to wild type values.

With increasing irradiance, NPQ rose in all plants, tending to saturate only at the highest irradiances measured (Fig. 6D). At low light (below 350 μmol m^{-2} s^{-1}), NPQ was similar in all three plants. At higher light intensities, however, a clear divergence in NPQ emerged.

Table 1
Quenching relaxation analysis of plants illuminated at high light

Measurement	Wildtype	*psad1-1*	*psael-3*
20% O_2 and 2000 μl l^{-1} CO_2			
NPQ_s	0.188 ± 0.005	0.610 ± 0.098	0.406 ± 0.038
NPQ_f	1.949 ± 0.068	2.433 ± 0.110	2.430 ± 0.204
NPQ_{total}	2.137 ± 0.073	3.043 ± 0.026	2.836 ± 0.171
Φ_{PSII}	0.175 ± 0.003	0.105 ± 0.002	0.114 ± 0.004
20% O_2 and 0 μl l^{-1} CO_2			
NPQ_s	0.398 ± 0.072	0.776 ± 0.085	0.572 ± 0.082
NPQ_f	2.170 ± 0.068	2.588 ± 0.067	2.533 ± 0.075
NPQ_{total}	2.568 ± 0.076	3.364 ± 0.078	3.105 ± 0.081
Φ_{PSII}	0.041 ± 0.002	0.037 ± 0.009	0.038 ± 0.008
2% O_2 and 2000 μl l^{-1} CO_2			
NPQ_s	0.143 ± 0.020	0.610 ± 0.092	0.327 ± 0.025
NPQ_f	1.917 ± 0.140	2.568 ± 0.068	2.530 ± 0.109
NPQ_{total}	2.060 ± 0.160	3.090 ± 0.120	2.857 ± 0.133
Φ_{PSII}	0.145 ± 0.010	0.090 ± 0.004	0.094 ± 0.007
Ratio Φ_{PSII} (2%/20%)	0.83	0.86	0.82

Values of the fast- and slow-relaxing components of NPQ (NPQ_f and NPQ_s, respectively) and Φ_{PSII} measured at 2000 μmol m^{-2} s^{-1} light at varying CO_2 and oxygen concentrations. Mean values ± SE of at least three measurements of wildtype, *psad1-1* and *psae1-3* plants are shown.

In *psad1-1* line, NPQ was clearly higher than in *psae1-3* line, which in turn was higher than in wildtype. A quenching relaxation analysis was conducted at high light to differentiate between NPQ as a pH-regulated protective process and photoinhibition (Table 1). The majority of quenching relaxed quickly in the dark (NPQ_f) in all plants, which is indicative of pH-dependence. However, a fraction of the quenching was more persistent (NPQ_s), suggesting that photoinhibition was occurring. The total NPQ_s was greater in the *psad1-1* and *psae1-3* lines, in particular in the former, suggesting greater susceptibility to photoinhibition in the knockout lines. Nevertheless, this damage only partially explained their elevated NPQ at high light. NPQ_f was also greater, and equally great in the two lines.

As in measurements of transiently induced NPQ at low light, the generation of ΔpH driving NPQ at high light might be related to cyclic electron flow or electron transport to oxygen. Quenching relaxation analysis was also carried out under low oxygen conditions (2%) to suppress electron transport to oxygen (Table 1). NPQ_{total} was similar to that recorded at 20% oxygen for all plants. Furthermore, the proportions of NPQ_s and NPQ_f were also similar. However, Φ_{PSII} values were slightly lower at depleted oxygen in all plants. This suggests that oxygen is a weak sink for electrons in all plant lines but that it is not a major contributor to net generation of ΔpH, as has been observed previously [27]. This contrasts to recent data published relating to cyanobacteria lacking PSI-E, where evidence for increased photoreduction of oxygen was presented [14].

Fig. 7 shows parameters relating to PSI photochemistry measured in the same leaves used in Fig. 6. In all plants, the proportion of P700 oxidised increased with increasing irradiances (Fig. 7A). At all irradiances, P700 was more oxidised in the wildtype than the *psad1-1* and *psae1-3* lines. Given that, in the two knockout lines, PSI has been reduced to limiting concentrations and there is therefore an excess of PSII turnover, the observation that PSI becomes oxidised with increasing irradiance is somewhat surprising. In the mutant lines, overall PSI content and activity is reduced, we do not expect electron flow to be limited on the acceptor side of PSI. The presence of an efficient sink for electrons seems to be sufficient to allow oxidation of P700 to occur. Given that the PSII acceptor pool becomes increasingly reduced at high light, this implies that, at high light, the slowest effective step in the electron transport chain must lie between PSII and PSI in all plants.

Upon a light–dark transition, P700 was reduced following a pseudo-first order decay, which can be fitted to an exponential equation to yield an apparent first order rate constant (k) [29] (Fig. 7B). This rate constant was similar in all three plants and constant throughout the irradiance range, except at 350 μmol m^{-2} s^{-1} where a lower value was attained in all plants. At lower light intensities, it was not possible to estimate k, due to the small signal size. The observation that k was not lowered in the mutant lines implies that the limitation in electron transport was not due to feedback regulation of the electron transport chain.

Multiplication of the rate constant for the re-reduction of P700, k, and the amount of oxidised P700 provides an estimate of PSI ETR, provided that at least 30% of PSI is oxidised [17,30]. In all plants, PSI ETR rose with increasing irradiance, across the irradiance range where PSI ETR could be estimated. In contrast, PSII ETR in the same irradiance range was saturated. This can be interpreted by stating that more electron transport is going through PSI than PSII at high light intensities, and that this is indicative of the occurrence of cyclic electron transport. Our data are in line with those previously reported at high light [27,28], where evidence for increased cyclic electron transport at high light has been reported. Thus, we conclude that cyclic electron transport is occurring at high light in both the *psad1-1* and *psae1-3* lines, in spite of the limitation of PSI.

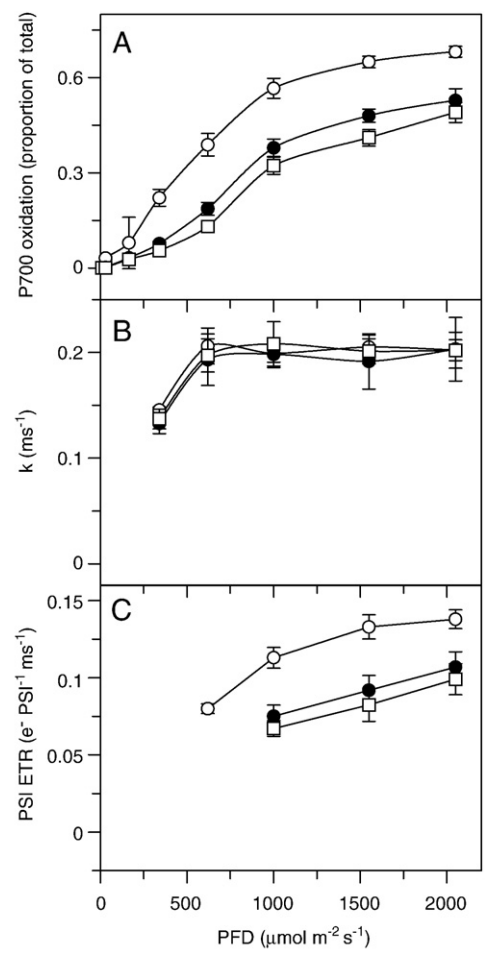

Fig. 7. Irradiance dependence of Photosystem I parameters in wildtype (○), *psad1-1* (●) and *psae1-3* (□) lines. The proportion oxidation of P700 (A) and the apparent rate constant for the re-reduction of PSI (k, B) were measured on leaves immediately after fluorescence measurements in Fig. 6. Values for k at lower irradiances (<350 μmol m^{-2} s^{-1}) are not shown as these could not be accurately measured, due to too low P700 oxidation. For conditions where >~15% PSI was oxidised, the rate of PSI turnover is estimated as ETR = $[P700^+]*k$. Each point represents the mean ± SE of at least three measurements on separate plants.

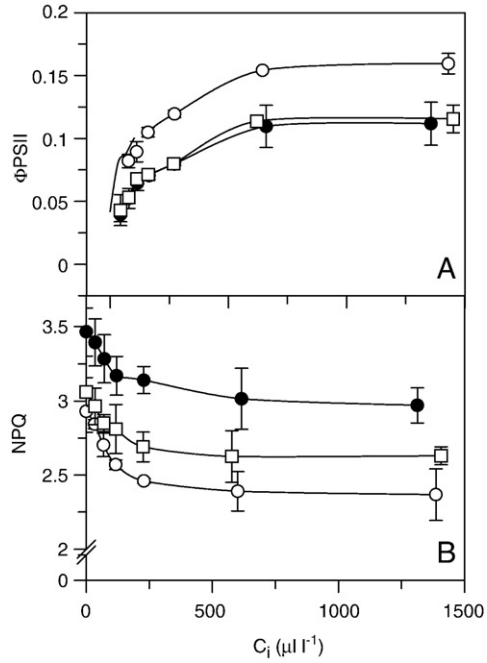

Fig. 8. Response of chlorophyll fluorescence quenching parameters to CO_2 concentration in wildtype (○), *psad1-1* (●) and *psae1-3* (□) lines. The quantum yield of PSII (A) and non-photochemical quenching (B) were measured in leaves subjected to a range of CO_2 concentrations at 20% oxygen and 1500 µmol m^{-2} s^{-1} white light. Fluorescence parameters were estimated as outlined in the legend for Fig. 1. Each point represents the mean ± SE of at least three measurements on separate plants.

3.5. Effect of lowering CO_2 availability on PSII and PSI electron transport

The occurrence of cyclic electron transport has been documented under drought conditions [17]. To investigate the effect of the limitation of CO_2 in the *psad1-1* and *psae1-3* lines, PSII photochemistry was measured at a range of different concentrations of CO_2 using chlorophyll fluorescence analysis (Fig. 8). Φ_{PSII} drops with decreasing CO_2 concentrations, reflecting a limitation of CO_2 supply to the Benson–Calvin cycle. In both *psad1-1* and *psae1-3* lines, Φ_{PSII} was lower than in wildtype plants at any CO_2 concentration (Fig. 8A). The degree of inhibition was similar in the two knockout lines. Notably, Φ_{PSII} converged to a similar value for all plants only at the very lowest CO_2 concentrations, even though CO_2, not PSI, is expected to be limiting for electron transport across a broader range of CO_2 concentrations.

Values of NPQ increased with decreasing concentrations of CO_2 in all plants (Fig. 8B). At all CO_2 concentrations, NPQ was higher for the *psad1-1* than for the *psae1-3* line, which in turn had higher NPQ than the wildtype. To investigate the nature of NPQ under CO_2 limitation, a quenching relaxation analysis at 0 µl l^{-1} CO_2 was carried out (Table 1). The additional NPQ at low CO_2 could be explained partly by photoinhibition and partly by accumulation of reversible quenching. NPQ_s was greatest in the *psad1-1* line, but was also elevated in the *psae1-3* relative to wildtype plants.

Fig. 9 shows parameters relating to PSI photochemistry measured in the same leaves used in Fig. 8. Decreasing concentrations of CO_2 resulted in increased oxidation of P700 in all cases (Fig. 9A). This increase was more pronounced in the *psad1-1* and *psae1-3* lines than the wildtype. At the highest CO_2 concentration, P700 oxidation was clearly higher for the wildtype, whereas, as the CO_2 concentration was decreased, values of P700 oxidation converged to similar high values for all three plants. At all CO_2 concentrations, the rate constant for reduction of P700, *k*, was similar in all plants (Fig. 9B). With decreasing CO_2 concentrations, *k* drops, reflecting the regulation of the electron transport chain [17]. Lowering of the CO_2 concentration resulted in values of *k* converging at a similar low value of approximately 0.05 in all plants. Under all conditions, the pool of oxidised P700 exceeds 30% allowing an estimation of PSI ETR [17,30]. In wildtype, PSI ETR fell with falling CO_2 concentration. For the mutant lines, PSI ETR was rather constant over a large range of CO_2 concentrations, only falling significantly at the lowest CO_2 concentrations (Fig. 9C).

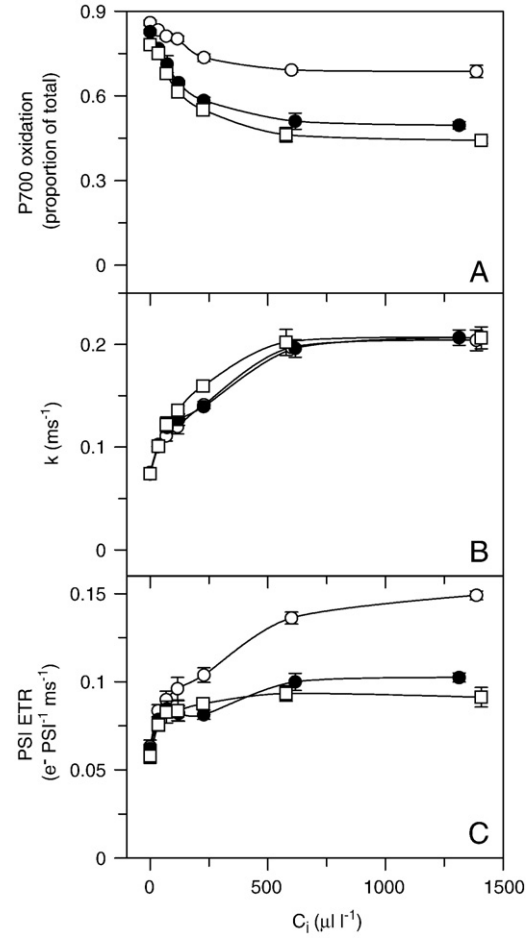

Fig. 9. Response of Photosystem I photochemistry to CO_2 in wildtype (○), *psad1-1* (●) and *psae1-3* (□) lines. The degree of oxidation of P700 (A), the rate constant for the re-reduction of PSI (B) and PSI electron transport rate (C) were made on leaves immediately after fluorescence measurements in Fig. 4. Each point represents the mean ± SE of at least three measurements on separate plants.

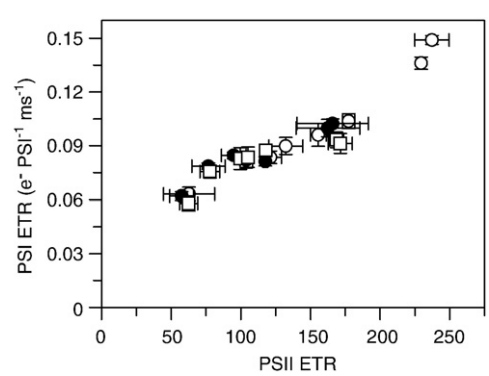

Fig. 10. Relationship between electron transport through PSI (PSI ETR), and PSII (PSII ETR) with varying CO_2 concentrations. Data points represent data collected at all CO_2 concentrations measured (taken from Figs. 8 and 9). Data for wildtype (○), *psad1-1* (●) and *psae1-3* (□) lines are shown.

An indication of the relative extent of cyclic electron transport can be obtained by comparing PSI and PSII ETR (Fig. 10). The low values for both PSII and PSI ETR correspond to the measurements at low concentrations of CO_2. In all plants, PSI ETR does not drop in proportion to PSII ETR with decreasing CO_2 concentrations. Golding and Johnson [17] provided evidence of down-regulation of linear but enhanced cyclic electron transport during drought or CO_2 limitation. In line with this, we demonstrate here that the lines lacking PSI-D1 and -E1 as well as wildtype plants have a capacity to increase cyclic electron transport, relative to linear, as a response to decreasing CO_2 concentrations.

4. Discussion

Without PSI-D1 or PSI-E1 PSI cannot be properly assembled — either they are not accumulated or the resulting protein has impaired function. The consequence of this is an imbalance in the stoichiometry of PSI to PSII in the favour of PSII. Thus, plants lacking PSI-D1 or PSI-E1 are expected to be PSI-limited. Several of the results presented in this paper cannot however be simply explained in terms of an imbalance in photosystem turnover. Indeed, the results presented here, lead us to suggest that PSI and PSII do not exist in a simple equilibrium but rather tend to support the idea proposed elsewhere [31] that distinct pools of PSI might exist that only partially interact.

At first analysis, at low light the *psad1-1* and *psae1-3* lines behave much as to be expected. Under such conditions, the turnover of each reaction centre will be determined largely by its antenna size. Thus a lowering in the concentration of PSI should give an imbalance in the ratio of PSI:PSII turnover, as is indeed observed. Plants might tend to compensate for such an imbalance either in the long term by altering the total amount of each photosystem or the antenna cross-section (i.e. making less LHCII and/or PSII and more LHCI) or dynamically via state transitions. It is clear that the former responses, if they are occurring, are not sufficient to compensate for the mutations. LHCII phosphorylation and migration to PSI are enhanced in mutant plants and do contribute towards balancing photosystem turnover, however these are again not sufficient to compensate for the overall loss of PSI activity (Fig. 2). Consistent with previous observations, we observe the presence of a stable pool of phosphorylated thylakoid proteins (Fig. 3), implying that even under pure far-red light where the PQ pool is fully oxidised, there is still a degree of activation of the STN7 kinase.

Previously, Finazzi et al. [21] described the occurrence of a transient non-photochemical quenching of chlorophyll fluorescence under conditions of a dark–light transition, which they ascribed to the generation of a large ΔpH, probably generated by cyclic electron transport or electron transport to oxygen, both of which involve PSI. The observation that this transient is enhanced in the PSI-deficient *psad1-1* and *psae1-3* lines is therefore somewhat surprising — a reduced amount of PSI should result in a reduced capacity to generate ΔpH. However, the observation that the competitiveness of cyclic electron transport is enhanced may explain this apparent anomaly. If, under conditions of limited electron flow, electrons are tending to feed back into the cyclic pathway in preference to being taken for the linear pathway, then it should be possible to generate a high ΔpH. This however only applies to conditions where the Benson–Calvin cycle is largely inactive. At steady state, the NPQ is no greater than in wildtype under low light conditions (Fig. 6). NPQ is not a direct indicator of ΔpH, since the sensitivity of quenching to the pH may vary between plants depending on xanthophyll content and light-harvesting (and PsbS) content, nevertheless, the occurrence of high NPQ is indicative of a high ΔpH being generated.

Under far-red light there is a net loss of electrons from PSI over time that is substantially slowed in the two mutants. The loss of electrons from PSI is likely to be a probabilistic event, whereby, with each charge separation, there is a certain probability that an electron will be lost. Increasing the irradiance will increase the rate of PSI turnover and therefore of loss of electrons from the PSI pool. The enhanced efficiency of cyclic flow implies that the probability of electrons being lost from PSI is lowered in the mutants. This suggests that the factor determining electron loss from cyclic is related to the ability of electrons to return to the electron transport chain, rather than the efficiency of stromal electron acceptors to remove them, consistent with the previous assertion that ferredoxin limits re-injection of electrons into the electron transport chain [32]. In the mutants, the total rate of charge separation in PSI will be lower, as the total amount of PSI is lowered. Therefore the return of electrons to the PSI donor side will less readily become limiting.

As light increased, the turnover of PSI remained limiting for linear electron transport in both mutant lines, as evidenced by the suppression of PSII ETR across all irradiances. If PSI and PSII existed in simple equilibrium, it should be expected that this would result in the PSI pool being maintained in a reduced state at all times. This is clearly not the case. Although the PSI pool is somewhat more reduced at any given irradiance, there remains a significant proportion that is oxidised, rising with rising irradiance. So, we can conclude that the turnover of at least a proportion of PSI is limited on the donor side. This might be explained as due to down-regulation of the cyt b_6f complex, as is seen, for example, at low CO_2. There is however no evidence that this is occurring. The rate constant for re-reduction of $P700^+$, k, is not lower in the mutant lines and does not fall with increasing irradiance. Rather, we suggest that a proportion of PSI might exist in rapid equilibrium with PSII and therefore be maintained in a reduced state at high light but that the remainder of PSI is uncoupled from linear electron transport and can therefore be oxidised under high light conditions. Overall, though, the proportion of PSI that is reduced under any conditions is higher in the wildtype than in the mutant lines, suggesting either that a larger proportion of PSI is accessible to PSII in the knockout lines or that the return of electrons via the cyclic pathway is more efficient, relative to PSI turnover. The latter proposal is consistent both with the low light response (Figs. 1,6,7) and also with the observation that NPQ is elevated at high light in the mutant lines (Fig. 6).

Under conditions of low CO_2, cyclic electron transport was enhanced in all plants, leading to an elevation of NPQ. PSII turnover was lowered across all CO_2 concentrations in the mutant lines whereas PSI turnover only fell significantly at the lowest CO_2 concentrations. The increased NPQ was not however sufficient to protect the knockout lines from photoinhibition at low CO_2, which was largely absent in the wildtype but substantial in the mutant lines. The observation that PSII turnover is lowered without there being a concomitant reduction in PSI turnover is consistent with PSI centres becoming uncoupled from PSII but being able to maintain their turnover as they switch to the cyclic pathway. This might reflect their location in the thylakoid membrane, e.g. a migration from granal to stromal membranes.

The relationship between PSII ETR and the rate of PSI turnover across a range of CO_2 concentrations is very similar in all plants (Fig. 10), however this does not mean that the absolute rate of cyclic electron transport is the same in all plants. The two knockout lines had an overall lower concentration of active PSI, so that the absolute rate of cyclic flow would have been lower. Nevertheless, in all cases, the rate of PSI turnover was largely maintained as PSII ETR fell, implying that cyclic flow was increasing in all cases.

In this study we had largely treated the two knockout lines as simply being reduced in PSI content, however this is probably a simplification as they do differ in the remaining content of PSI. Loss of PSI-D has been shown to result in a net loss of the core PSI complex, however this is not the case for mutants lacking PSI-E. Indeed, plants lacking both genes encoding PSI-E are able to grow autotrophically, albeit at a highly reduced rate [12]. The differences we see between the two lines (e.g. the flash-induced fluorescence quenching seen in Fig. 1) are probably explained as being due to there being a more severe loss of PSI activity in the *psad1-1* line than in *psae1-3*. We

cannot exclude that the remaining PSI centres in *psae1-3* do not have altered functionality, rather than simply impaired activity, however we have no evidence to indicate that this is the case. Further confirmation of this might come from examination of other mutants e.g. suppressed in core PSI polypeptides.

In conclusion, the data we have presented here suggest that there is no simple equilibrium between PSII and PSI, but rather that a proportion of PSI exists that is not readily reduced by PSII. Furthermore we suggest that cyclic electron flow tends to out-compete linear flow under conditions where PSI is limiting.

Acknowledgements

We would like to thank Mr. John Simpson for his help in developing LED light drivers and Mr. Kevin Crawford and Dr. Rachel Webster for their help and support and Ms. Beena Nandha, Prof. Pierre Joliot (IBPC, Paris), Dr. Giovanni Finazzi (IBPC, Paris) and Dr. Paolo Pesaresi (University of Milan) for useful discussions. We acknowledge the UK Biotechnology and Biological Sciences Research Council, grant no. BB/C508877/1 to GNJ/PG.

References

[1] P.E. Jensen, R. Bassi, E.J. Boekema, J.P. Dekker, S. Jansson, D. Leister, C. Robinson, H.V. Scheller, Structure, function and regulation of plant photosystem I, Biochim. Biophys. Acta 1767 (2007) 335–352.
[2] A.H. Mehler, Studies on reactions of illuminated chloroplasts. I. Mechanism of the reduction of oxygen and other Hill reagents, Arch. Biochem. Biophys. 33 (1951) 65–77.
[3] U. Heber, Irrungen, Wirrungen? The Mehler reaction in relation to cyclic electron transport in C3 plants, Photosynth. Res. 73 (2002) 223–231.
[4] P. Joliot, A. Joliot, Cyclic electron flow in C3 plants, Biochim. Biophys. Acta 1757 (2006) 362–368.
[5] G.N. Johnson, Cyclic electron transport in C-3 plants: fact or artefact? J. Exp. Bot. 56 (2005) 407–416.
[6] R.M. Mannan, H.B. Pakrasi, K. Sonoike, The Psac protein is necessary for the stable association of the Psad, Psae, and Psal proteins in the photosystem-I complex — analysis of a cyanobacterial mutant strain, Arch. Biochem. Biophys. 315 (1994) 68–73.
[7] A. Ihnatowicz, P. Pesaresi, C. Varotto, E. Richly, A. Schneider, P. Jahns, F. Salamini, D. Leister, Mutants for photosystem I subunit D of *Arabidopsis thaliana*: effects on photosynthesis, photosystem I stability and expression of nuclear genes for chloroplast functions, Plant J. 37 (2004) 839–852.
[8] A. Haldrup, C. Lunde, H.V. Scheller, *Arabidopsis thaliana* plants lacking the PSI-D subunit of photosystem I suffer severe photoinhibition, have unstable photosystem I complexes, and altered redox homeostasis in the chloroplast stroma, J. Biol. Chem. 278 (2003) 33276–33283.
[9] C. Varotto, P. Pesaresi, J. Meurer, R. Oelmuller, S. Steiner-Lange, F. Salamini, D. Leister, Disruption of the *Arabidopsis* photosystem I gene psaE1 affects photosynthesis and impairs growth, Plant J. 22 (2000) 115–124.
[10] P. Pesaresi, C. Lunde, P. Jahns, D. Tarantion, J. Meurer, C. Varotto, R.D. Hirtz, C. Soave, H.V. Scheller, F. Salamini, D. Leister, A stable LHCII-PSI aggregate and suppression of photosynthetic state transitions in the psae1-1 mutant of *Arabidopsis thaliana*, Planta 215 (2002) 940–948.
[11] A. Ihnatowicz, P. Pesaresi, K. Lohrig, D. Wolters, B. Muller, D. Leister, Impaired photosystem I oxidation induces STN-7-dependent phosphorylation of the light harvesting complex I protein Lhca4 in *Arabidopsis thaliana*, Planta 227 (2008) 717–722.
[12] A. Ihnatowicz, P. Pesaresi, D. Leister, The E subunit of photosystem I is not essential for linear electron flow and photoautotrophic growth in *Arabidopsis thaliana*, Planta 226 (2007) 889–895.
[13] L. Yu, J.D. Zhao, U. Muhlenhoff, D.A. Bryant, J.H. Golbeck, Psae is required for in-vivo cyclic electron flow around photosystem-I in the cyanobacterium *Synechococcus* sp. Pcc-7002, Plant Physiol. 103 (1993) 171–180.
[14] R. Jeanjean, A. Latifi, H.C.P. Matthijs, M. Havaux, The PsaE subunit of photosystem I prevents light-induced formation of reduced oxygen species in the cyanobacterium *Synechocystis* sp. PCC 6803, Biochim. Biophys. Acta 1777 (2008) 308–316.
[15] C. Breyton, B. Nandha, G.N. Johnson, P. Joliot, G. Finazzi, Redox modulation of cyclic electron flow around photosystem I in C3 plants, Biochemistry 45 (2006) 13465–13475.
[16] K. Maxwell, G.N. Johnson, Chlorophyll fluorescence — a practical guide, J. Exp. Bot. 51 (2000) 659–668.
[17] A.J. Golding, G.N. Johnson, Down-regulation of linear and activation of cyclic electron transport during drought, Planta 218 (2003) 107–114.
[18] P. Joliot, A. Joliot, Cyclic electron transfer in plant leaf, Proc. Nat. Acad. Sci. U. S. A. 99 (2002) 10209–10214.
[19] C. Lunde, P.E. Jensen, A. Haldrup, J. Knoetzel, H.V. Scheller, The PSI-H subunit of photosystem I is essential for state transitions in plant photosynthesis, Nature 408 (2000) 613–615.
[20] V. Bonardi, P. Pesaresi, T. Becker, E. Schleiff, R. Wagner, T. Pfannschmidt, P. Jahns, D. Leister, Photosystem II core phosphorylation and photosynthetic acclimation require two different protein kinases, Nature 437 (2005) 1179–1182.
[21] G. Finazzi, G.N. Johnson, L. Dallosto, P. Joliot, F.A. Wollman, R. Bassi, A zeaxanthin-independent nonphotochemical quenching mechanism localized in the photosystem II core complex, Proc. Nat. Acad. Sci. U. S. A. 101 (2004) 12375–12380.
[22] J.F. Allen, Protein-phosphorylation in regulation of photosynthesis, Biochim. Biophys. Acta 1098 (1992) 275–335.
[23] A. Haldrup, P.E. Jensen, C. Lunde, H.V. Scheller, Balance of power: a view of the mechanism of photosynthetic state transitions, Trends Plant Sci. 6 (2001) 301–305.
[24] A. Ihnatowicz, P. Pesaresi, K. Lohrig, D. Wolters, B. Muller, D. Leister, Impaired photosystem I oxidation induces STN-7-dependent phosphorylation of the light harvesting complex I protein Lhca4 in *Arabidopsis thaliana*, Planta 227 (2008) 717–722.
[25] K. Siebke, A. Laisk, S. Neimanis, U. Heber, Evidence that NADP-dependent glyceraldehydephosphate dehydrogenase, but not ferredoxin-NADP reductase, controls electron flow to phosphoglycerate in the dark-light transition, Planta 185 (1991) 337–343.
[26] P. Joliot, A. Joliot, Cyclic electron transport in plant leaf, Proc. Nat. Acad. Sci. U. S. A. 99 (2002) 10209–10214.
[27] J.E. Clarke, G.N. Johnson, In vivo temperature dependence of cyclic and pseudocyclic electron transport in barley, Planta 212 (2001) 808–816.
[28] C. Miyake, Y. Shinzaki, M. Miyata, K. Tomizawa, Enhancement of cyclic electron flow around PSI at high light and its contribution to the induction of non-photochemical quenching of chl fluorescence in intact leaves of tobacco plants, Plant Cell Physiol. 45 (2004) 1426–1433.
[29] T. Ott, J. Clarke, K. Birks, G. Johnson, Regulation of the photosynthetic electron transport chain, Planta 209 (1999) 250–258.
[30] A.J. Golding, G. Finazzi, G.N. Johnson, Reduction of the thylakoid electron transport chain by stromal reductants — evidence for activation of cyclic electron transport upon dark adaptation or under drought, Planta 220 (2004) 356–363.
[31] P.A. Albertsson, The structure and function of the chloroplast photosynthetic membrane — a model for the domain organization, Photosynth. Res. 46 (1995) 141–149.
[32] H. Yamamoto, H. Kato, Y. Shinzaki, S. Horiguchi, T. Shikanai, T. Hase, T. Endo, M. Nishioka, A. Makino, K. Tomizawa, C. Miyake, Ferredoxin limits cyclic electron flow around PSI (CEF-PSI) in higher plants-stimulation of CEF-PSI enhances non-photochemical quenching of Chl fluorescence in transplastomic tobacco, Plant Cell Physiol. 47 (2006) 1355–1371.